Characterization of Bottom Ash Waste Adsorbent from Palm Oil Plant Boiler Burning Process to Adsorb Carbon Dioxide in a Fixed Bed Column

Novi Sylvia[1,2], Fitriani Fitriani[2], Rozanna Dewi[2], Rizka Mulyawan[2], Abrar Muslim[3], Husni Husin[3], Yunardi Yunardi[3*], and Mutia Reza[4]

[1]*Doctoral Program, School of Engineering, Post Graduate Program, Universitas Syiah Kuala, Banda Aceh 23111, Indonesia*

[2]*Department of Chemical Engineering, Malikussaleh University, Lhokseumawe, 24351, Indonesia*

[3]*Department of Chemical Engineering, Universitas Syiah Kuala, Banda Aceh 23111, Indonesia*

[4]*Department of Chemical Engineering, Institut Teknologi Kalimantan, Indonesia*

Corresponding author:

email: yunardi@unsyiah.ac.id

Received: June 10, 2021
Accepted: September 18, 2021

DOI: 10.22146/ijc.66509

Abstract: *Palm oil bottom ash utilization from mill boilers as CO_2 adsorbent has been in use for few years. This study aims to examine adsorbent characteristics and capabilities of bottom ash produced from boiler combustion in palm oil industry for CO_2 adsorption before and after utilization, such as compound functional group using the Fourier Transform Infra-Red (FT-IR) spectrophotometer, adsorbent morphology through Scanning Electron Microscopy (SEM), and compound amount using Energy Dispersive X-Ray Spectroscopy (EDX). The CO_2 adsorption was carried out in fixed-bed column. Process variables consist of volumetric flow rate, contact time and bed height. Results showed that SiO_2 compounds in the heterogeneous form with average particle size of 1073 nm, as supported by FT-IR spectrum finding indicating SiO_2 signal at wavelength of 958–954 cm^{-1}. Additionally, EDX analysis showed Silica and Oxygen content of 11.88% and 36.90%, resulting 70% CO_2 adsorption capacity of 0.350 mg/g at discharge of 5 L/min, contact time of 40 min, and bed height of 12 cm. Langmuir isotherm model was obtained with R^2 of 0.998, q_m of 1.588, and k_L of 0.144. Meanwhile, the kinetic model followed a simple first-order prototypical with R^2 of 0.952, $C0_2$ of 0.260, and k_1 of 0.006.*

Keywords: *adsorption; adsorbent; bottom ash; CO_2 gas; fixed-bed column*

■ INTRODUCTION

Global warming from climate change has been considered a severe issue in the last decades. Several types of research related to climate change show an increase in the Earth's temperature due to human activities [1]. Various human activities such as deforestation, industrial waste smoke, vehicle smoke, and others have caused greenhouse gas emissions to the atmosphere; hence, solar radiation is trapped and increases the Earth's average temperature [2-3]. Numerous efforts have been developed to absorb carbon dioxide (CO_2) to decrease the greenhouse gas effect [4]. The Indonesian government is also aware of the issue and commits to reducing greenhouse gas emissions [5]. In the Conference of Parties (COP) 21 on United Nations Framework about Climate Change (UNFCCC) in Paris, France, 30 November 2015, President Joko Widodo stated Indonesia's commitment to reduce greenhouse gas emissions in the amount of 29% by nation effort and 41% through international support until 2030.

Indonesia also has a national action plan to reduce greenhouse gas emissions as in Presidential Decree No. 61 of 2011 on the National Action Plan on Greenhouse Gas Emission and Presidential Decree No. 71 of 2011 on implementing a National Greenhouse Gases Inventory. The inventory shows that industrial activity is one of the primary sources of greenhouse gas (GHG) emissions is CO_2 [6-7]. More than 75% of GHG composition in the atmosphere is CO_2. Currently, CO_2 concentration has risen from 280 ppm in the pre-industrial period to be

400 ppm. Meanwhile, the recommended limit is 350 ppm. Therefore if CO_2 contribution in diverse activities is significantly reduced, then the global warming effect to climate change can be suppressed [8].

Several methods to handle CO_2 gas emissions have been reported, including physical and chemical absorption, cryogenic, separation with membrane, microalga bio-fixation, and adsorption [9-10]. Among the mentioned methods, the most commonly applied method is the absorption method using an amine functional group compound, in which a gas component is separated from a gas mixture by passing it through liquid [11-13]. However, there are drawbacks in this separation process like amine mixture degradation due to impurities in the gas phase at low temperature (below 50 °C), apparatus corrosion, the extensive energy requirement for regeneration, solvent quality degradation due to impregnation with other products, and amine escape by vaporization [14].

The adsorption method is preferable to the absorption method due to adsorption is more economical, able to remove organic materials, and no poisonous side effects occur [15]. Furthermore, the adsorption method is a promising alternative to adsorb CO_2, considering its relatively inexpensive, more straightforward process and no liquid waste produced [4]. Many reports have discussed several types of research on different adsorbents for the adsorption CO_2 process, namely activated carbon, zeolite, silica mesopores, alumina, double-layered hydroxide, and metal oxide. A summary of the adsorption capacity reported for employing various types of adsorbents is presented in Table 1.

Biomass and waste-based adsorbent materials are usually preferable for commercial purposes, namely solid waste from palm oil plants, palm shells, and husk [16]. Many plants utilize shell and husk as fuel to boiler producing steam. Palm shell and husk burning liberate ash left at the furnace as solid granules or crust, usually called bottom ash. Bottom ash contains silica (SiO_2) and alumina (Al_2O_3), which is the primary content of zeolite. Zeolite has adsorption selectivity CO_2/N_2 5 to 10 times higher than carbon-based adsorbent in fixed-bed columns [3,12,17]. Bottom ash has the same content as zeolite; hence it can absorb CO_2.

Studies on bottom ash-based adsorbents have been done to adsorb heavy metals but are still limited for CO_2 adsorption. Currently, the utilization of bottom ash is not optimum and well managed yet. Bottom ash is an issue in the palm oil industry since the storage occupies a large area, increasing annually [18]. Laharto et al. [16] used the synthesis of mesoporous silica from bottom ash waste for CH_4 adsorption. The adsorption capacity at a pressure of 1 atm and a temperature of 30 °C is 0.923 mmol/g. Lira-Zúñiga et al. [17] used biomass combustion ashes on agricultural to CO_2 adsorption. The bottom ash sample from the combustion of wheat bran (agricultural biomass) and its pellets showed a higher adsorption capacity for most of the temperatures studied. The pelletized bottom ash reached the maximum adsorption capacity (0.07 mmol CO_2/g), followed by the non-pelletized bottom ash (0.06 mmol CO_2/g).

By considering the above concern, this research is aimed to study the characteristics and capability of bottom ash from the palm oil industry burning in the boiler as adsorbent to adsorb CO_2. Adsorption is conducted at the fixed-bed column. Previous studies using this absorbent to absorb CO_2 have been done [5,8,14]. However, variation of the flow rate and bed height has not been studied yet. Therefore, this research

Table 1. The adsorption capacity of diverse adsorbents

Adsorbent	Temperature (°C)	Pressure (atm)	Adsorption capacity (mmol/g)	References
Activated Carbon	25	1	1.202	[13]
Activated Carbon	50	1	0.450	[14]
Activated Carbon	25	1	2.828	[15]
Zeolite 13 X	25	1	4.245	[15]
Zeolite 4A	25	1	3.263	[15]

focuses on various volumetric flow rates, contact times, and bed heights. Adsorption equilibrium is generally studied through the adsorption isotherm approach [19]. In this study, the Langmuir and Freundlich adsorption equilibrium models were evaluated. The effectiveness of the adsorption in a fixed-bed column using bottom ash as adsorbent is then examined.

■ EXPERIMENTAL SECTION

Materials

The raw material that was used in this research was bottom ash from boiler burning of Palm Oil Plant PT. Syaukad Sejahtera, Kuta Blang, Gerugok, North Aceh, Indonesia and it was used as adsorbent. The supporting raw material was tapioca flour (SMS Genigel 48 Modified) and distilled water as a mixture for making tapioca glue.

Instrumentation

The adsorbent is applied at the acrylic pipe as an adsorption column with a 6.4 cm diameter and 30 cm length, as shown in Fig. 1, done at a single column. Additional used apparatuses were oven (Memmert UN 30), valve (VG 16 DD), hot plate (Heidolph C-MAG MS 4), sieve mesh 20 mesh (AMB No 20), adsorbent mold (tube mold stainless steel 1.5 × 1 cm), furnace (FNC-2 B-One Furnace), desiccator, spatula, beaker glass 500 mL, measuring cup 100 mL, porcelain cup, CO_2 tube detector from China (HT-2000 CO_2 meter), Scanning electron microscope/energy-dispersive X-ray spectroscopy (SEM/EDX, CARL ZEISS type EVO MA 10), X-Ray Diffraction (XRD, Shimadzu XRD-6100), and Fourier Transform Infra-Red spectrophotometer (FT-IR, IR Prestige 21).

Procedure

The raw palm kernel shell was washed with deionized water several times to remove all traces, such as oil and dirt. Next, the material was dried in an oven with a temperature of 100 °C. The preparation process was initiated by sieving 100 g of bottom ash using a 20 mesh sieve. Then 15 g of tapioca flour and 45 mL of distilled water are heated until they become glue. Furthermore, 100 g of bottom ash and the glue are mixed and stirred until evenly distributed. Next, the mixture was printed using a 1.5 cm diameter mold with a thickness of 1 cm then dry in the oven for 2 h using a temperature of 105 °C. After that, the mixture was calcinated with a furnace at 600 °C for 120 min. The adsorbent is then cooled using a desiccator to room temperature and ready for the CO_2 absorption process.

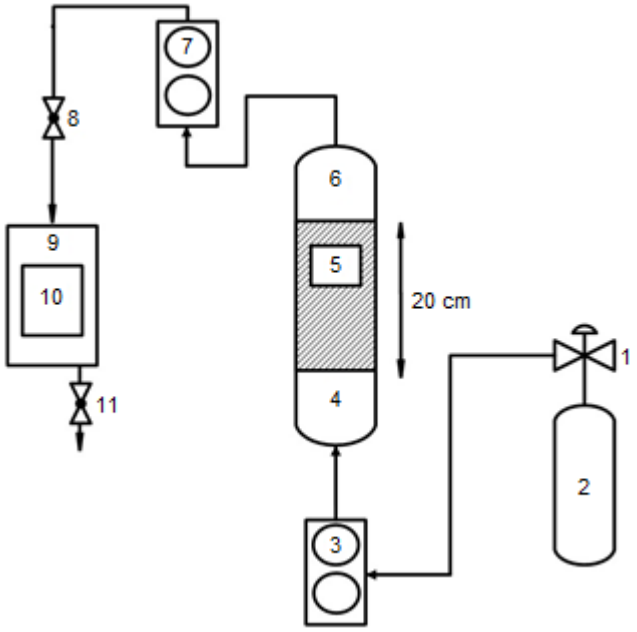

Fig 1. Single column adsorption column diagram of experimental apparatus for fixed-bed adsorption: (1) valve; (2) CO_2 gas cylinder; (3) flow meter CO_2 in; (4) bottom column adsorption (5) fixed-bed adsorber; (6) top column adsorption; (7) flowmeter CO_2 out; (8) valve; (9) box detector gas (10) CO_2 analyzer; (11) stop valves

The adsorption process was initiated by flowing CO_2 (C_0) 500 ppm into an adsorption column. First, the bottom ash adsorbent used was placed in a column of 30 cm and 6.4 cm in diameter, whereas the height of adsorbent (Z) in a column was varied of 4 cm (14 g), 8 cm (28), and 12 cm (42 g). Next, CO_2 was flown into a column with flow rates 10, 15, and 20 L/min and varied contact times of 10, 20, 30, and 40 min, as shown in Fig. 1. After that, the efficiency and adsorption capacity of CO_2 was calculated with the following Eq. (1) and (2) [5,14]:

$$\text{Efficiency} = \frac{CO_{2\ \text{Initial}} - CO_{2\ \text{Final}}}{CO_{2\ \text{Initial}}} \times 100\% \quad (1)$$

$$\text{Adsorption Capacity} = \frac{\text{Flowrate } (CO_{2\ \text{Initial}} - CO_{2\ \text{Final}})}{\text{Sample Mass}} \quad (2)$$

■ RESULTS AND DISCUSSION

This activation is purposed to switch cations to be H^+ and release Al, Fe, Mg, and other impurities (containing alkaline/alkaline Earth) from the structural grid. Impurities on the adsorbent surface covering active sites of adsorbent can be removed by burning during activation. As a result, the adsorbent structure has a broader area and improves the active site, exposing covered active sites and new active site occurrence. In addition, the surface area specified pores improvement and the active sites enable adsorption capability enhancement. The CO_2 adsorption mechanism is shown in Fig. 2.

Adsorbent Characterization

FT-IR analysis

FT-IR measurement results in the form of the spectrum before and after adsorption is shown in Fig. 3. Peaks appeared identifies several functional groups. The peak at wave number 3387–3010 cm^{-1}, stretching vibration from the OH group, showed water in the sample. The peak affirms this interpretation at 1629–1504 cm^{-1} from the –OH group's bending vibration. The peak at 958–954 cm^{-1} showed the Si–O–Si group that identified silica in the bottom ash. The other peaks are at 812 cm^{-1}, showing the Al–O–Al group of alumina and at 505 cm^{-1} for the Si–O–Al adsorption band. Finally, CO_2 gas adsorption is shown at 2337 cm^{-1}. This result is suitable to adsorbing peak reported by other researchers who showed adsorbing band of CO_2 in the range of 2500–2000 cm^{-1} [16-19].

SEM/EDX analysis

SEM/EDX Analysis was to comprehend the bottom ash adsorbent characteristic before and after adsorption. SEM testing was applied to observe the morphology or material surface description and EDX to analyze the adsorbent's material components or atomic composition. The SEM analysis result can be seen in Fig. 3 and 4.

Fig. 4 shows bottom ash SEM results before adsorption that had been physically activated with activation temperature 600 °C, causing reduction of water molecules and organic materials from pore channels, increasing the number of pore volume and adsorbent surface area. The average pore size is 767 nm.

Fig. 4 shows the adsorbent SEM after adsorption, it can be seen that the pore diameter became varied, and the pore hollows became tighter with an average diameter

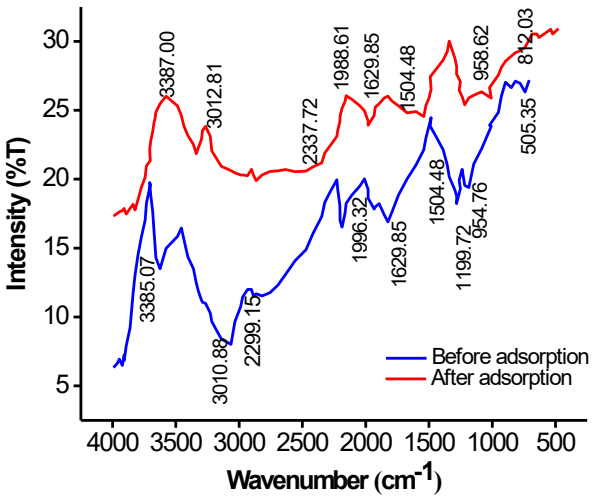

Fig 3. Bottom ash FT-IR result

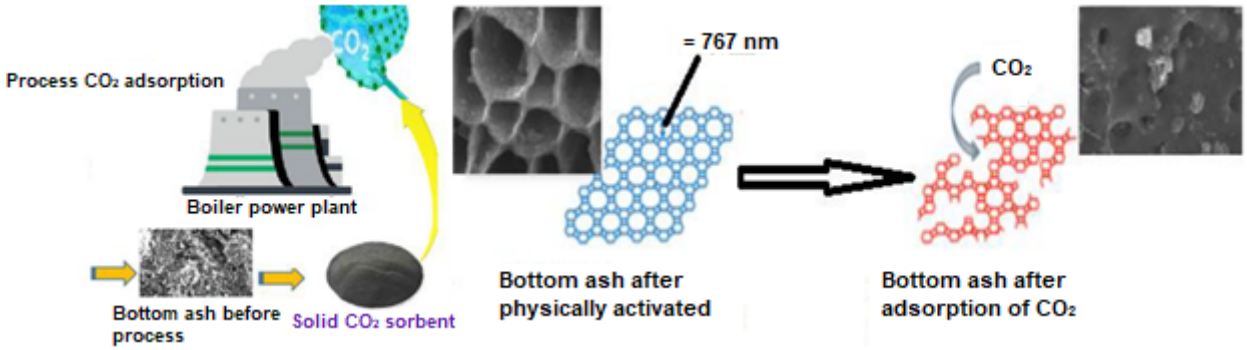

Fig 2. Carbon dioxide adsorption mechanism

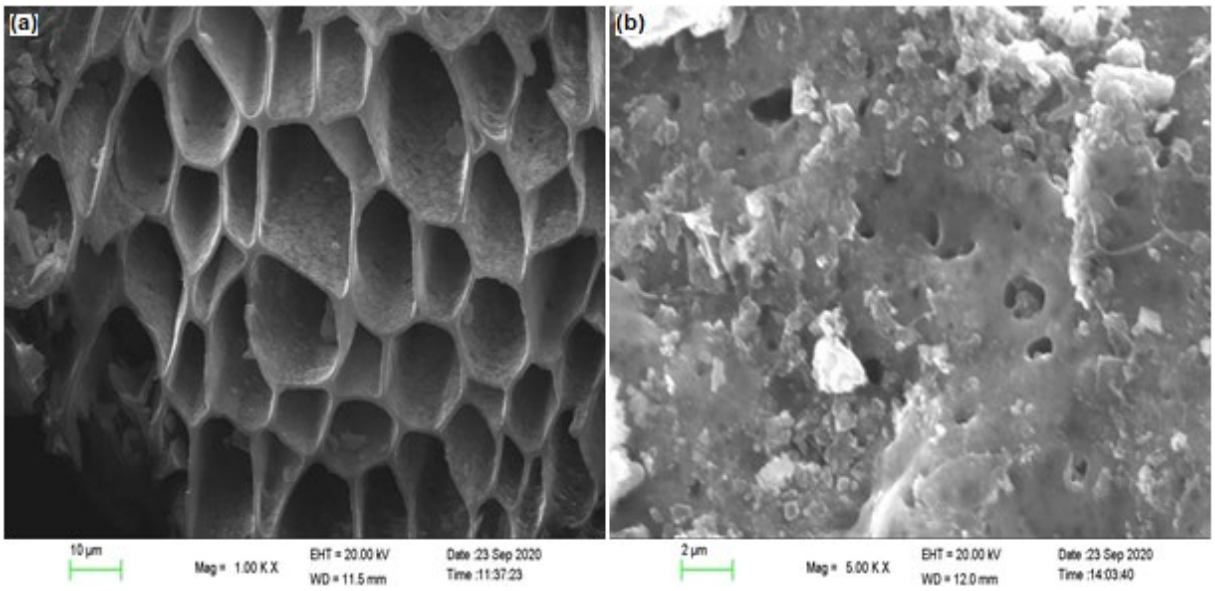

Fig 4. Adsorbent SEM result (a) before and (b) after adsorption

after adsorption 564 nm. The pore diameter became hollows because CO_2 gas was adsorbed so that adsorbent pores were covered and bound. SEM analysis shows that the adsorbent based on the bottom ash of the palm oil plant had a pore size of more than 50 nm. According to the size, the adsorbent is classified as macropores typed adsorbent and suitable as reported by other literature stating that POFA has three types; macropore (55 nm and > 55 nm), mesopore (7 nm and 8 nm), and micropore (< 1 nm) [2].

The bottom ash EDX analysis result is shown in Fig. 5 and Table 1. Table 1 shows that bottom ash components are C, O, Mg, Al, Si, P, S, K, Ca, and Fe elements. The highest composition components were carbon, oxygen, and silica, identifying that bottom ash has silica oxide (SiO_2) as an adsorbent composing component. The EDX analysis result fits with the XRD characteristics result and demonstrates the same composing elements. SiO_2 is proven to have good activity in the adsorption process.

Effect of flow rate on the breakthrough curve. The breakthrough curve for a column was determined by plotting the ratio of C_t/C_0 against time, as shown in Fig. 5. The column was found to perform effectively at the lowest rate of 5 L/min. Previously, breakthrough and exhaustion were reached at a flow rate of 5 to 20 L/min. The column

Table 1. Adsorbent EDX analysis results before adsorption and after adsorption

No	Element	Atom (%)		
		Bottom ash	Before Adsorption	After Adsorption
1	C	40.35	45.77	69.02
2	O	36.29	36.90	23.63
3	Mg	1.21	1.01	0.90
4	Al	0.42	0.36	0.10
5	Si	7.68	11.88	1.84
6	P	0.63	0.55	0.31
7	S	0.56	-	0.19
8	K	0.39	1.88	1.79
9	Ca	7.47	1.36	1.63
10	Fe	0.44	0.28	0.07
11	Cl	0.42	-	-

breakthrough time ($C_t/C_0 = 0.05$) was reduced from 150 min to 10 min by flow rate was increasing between 5 to 20 L/min. The decline of contact time has limited the contact of CO_2 against bottom ash CO_2 did not have sufficient time to diffuse into the pores of bottom ash at a higher flow rate, and CO_2 was out of the column before equilibrium. Similar results were found in the adsorption of CO_2 of the fixed-bed system in the column [20].

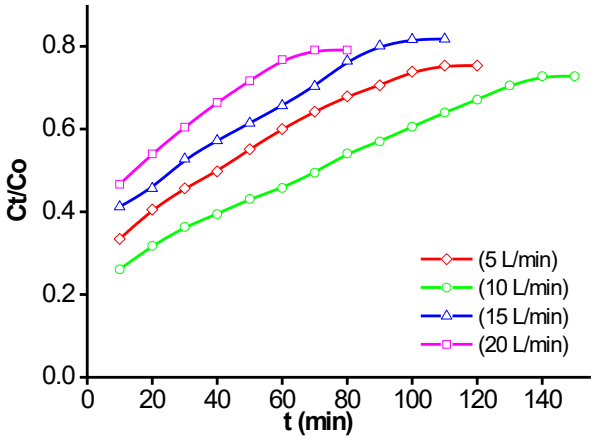

Fig 5. Breakthrough curves: the effect of flow rate on CO_2 adsorption (C_0 = 500 mg/L and Z = 12 cm)

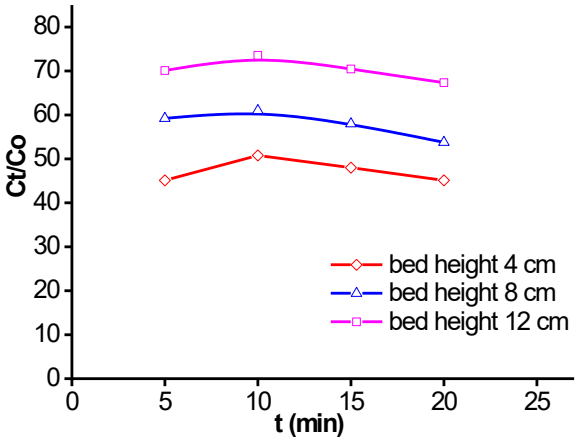

Fig 6. Correlation between flow rate and CO_2 adsorption efficiency graph at different bed height

Effects of flow rate, contact time, and bed height to CO_2 adsorption efficiency and adsorption capacity. CO_2 flow rate and bed height have significant effects on adsorption efficiency. Fig. 6 shows that a greater flow rate yielded a lower adsorption efficiency. The highest adsorption efficiency was at 10 L/min flow rate and bed height 12 cm. As the flow rate of CO_2 is getting higher, the contact time between CO_2 and adsorbent becomes shorter, thus the less CO_2 adsorption efficiency percentage [20]. These results are proportional to reported research from several works of literature that the flow rate significantly affects the adsorption process [21].

Contact time and collision are essential factors in adsorption. According to collision theory, the rate of reaction is the number of collisions in the time unit. The longer the contact time, the more collisions occur, hence the faster chemical reaction to reach equilibrium. The duration needed to achieve adsorption equilibrium are different. The type of interaction between adsorbent and adsorbate has influenced the result. The influence of contact time on the efficiency of adsorbent adsorbs CO_2 gas is shown in Fig. 7.

Fig. 7 shows the adsorption contact time started from 10 to 40 min. The best contact time took place at 40 min alongside the highest adsorption efficiency of 70% at 12 cm of bed height. The ability of the adsorbent declined after the twentieth minute implied that the adsorbent was saturated after that period because the adsorbent surface has a certain number of active adsorption sites. The

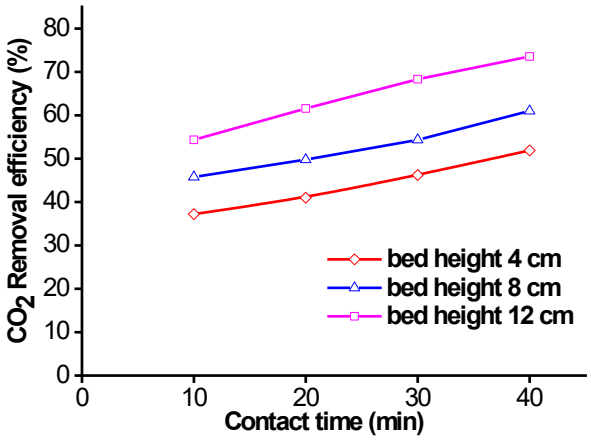

Fig 7. Correlation between contact time and CO_2 adsorption efficiency graph at different bed heights

number of active sites is proportional to the adsorbent surface area. The active site is the adsorbate attaching media on the adsorbent surface. After some time, the active site becomes saturated, and desorption occurs, the detachment of adsorbed molecules on the surface. Thus, after the twentieth-minute desorption happened in which the adsorbed molecules were detached, the CO_2 composition increased, or CO_2 adsorption efficiency declined.

Effects of contact time and bed height to adsorption capacity. Determination of adsorption capacity was done to understand the bottom ash capability in adsorbing CO_2. The effects of contact time and bed height on adsorption capacity are shown in Fig. 8.

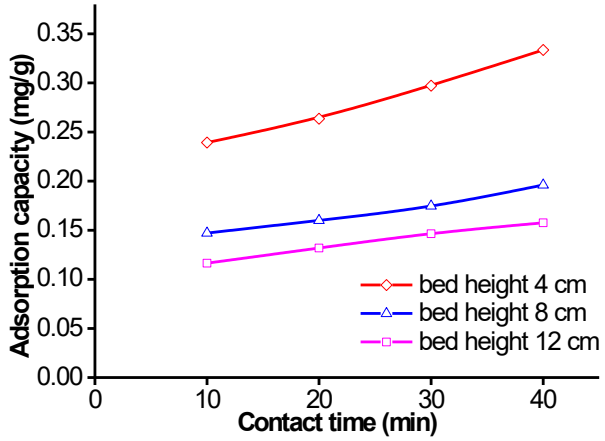

Fig 8. Contact time to adsorption capacity relation graphs at different bed height

Fig. 8 shows that the adsorption capacity increases as the bed height increases. The increment can be correlated with adsorbent surface area and its active sites. The higher bed height means the larger surface area of adsorbent to more CO_2 adsorption capacity [22]. The highest adsorption capacity was 0.350 mg/g was achieved at a contact time of 40 min and bed height 4 cm. At the beginning of contact time, the adsorption process took place at a fast rate since the active site of the adsorbent was still large so that the binding of adsorbate molecules frequency became sufficiently high. As the contact time increases, the amount of adsorbate adsorbed to the adsorbent surface becomes higher until the equilibrium point is reached. Excessive contact time between adsorbent and adsorbate causes adsorbent to be saturated and detached from adsorbate [23-25].

Isothermal Adsorption

Adsorption equilibrium, which is generally studied through the adsorption isotherm approach, is an essential foundation for understanding an adsorption process, especially for finding out how many adsorbate molecules can be adsorbed by a porous material. The adsorption equilibrium model for pure components was based on Langmuir's [14-15] theory about monolayer adsorption on an ideal surface. Langmuir and Freundlich's models are used to represent data adsorption balance. Langmuir's model assumes that the adsorbent surface is homogeneous where the constant energy adsorption on the entire surface of the adsorbent. This model also assumes that the adsorption is localized, and each location can only accommodate one molecule or atom. Adsorption isotherms Freundlich and Langmuir of CO_2 are shown in Table 2. A suitable isotherm model for the equilibrium curve must be determined to optimize the design of the sorption system for the absorption of CO_2 in bottom ash. In this study, the balance model that has been analyzed is Langmuir and Freundlich. The predicted value of the model and the experimental data was validated by comparing the experimental adsorption capacity with the adsorption capacity estimated by this model via a coefficient of determination (R^2, value close to or equal to 1) [19-20], shown in Fig. 9.

Table 2. Parameter isotherm Langmuir and Freundlich for adsorption CO_2 in bottom ash

Type	Parameters	Unit	Equation non-Linear
Langmuir			
q_m	1.588	mg/g	$q = \frac{q_m k_L C_e}{1 + k_L C_e}$
k_L	0.144	-	
R^2	0.998	-	
Freundlich			
k_F	6.519	-	$q = k_f C_e^{\frac{1}{n}}$
n	-1.812	-	
R^2	0.815	-	

where: q is the amount of adsorbed CO_2 per unit weight of bottom ash at equilibrium, and C_e is the unadsorbed CO_2 concentration in effluent at equilibrium (mg/L). k_L is the Langmuir equilibrium constant, q_m is the amount of CO_2 adsorbed with monolayer coverage, k_F is the Freundlich constant, and n is the Freundlich exponent

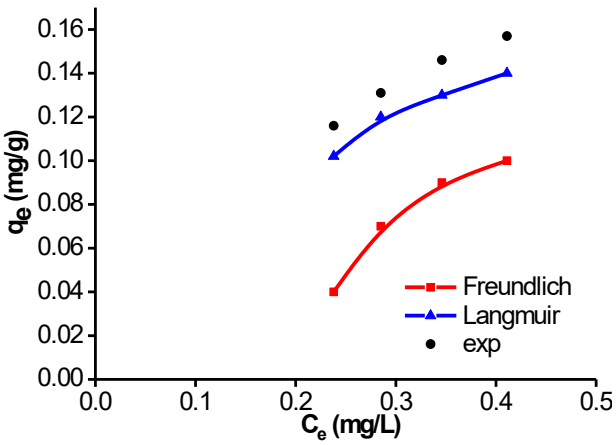

Fig. 9. Contact time to adsorption capacity relation graphs at different bed height

Table 3. Parameter kinetic models for adsorption CO_2 in bottom ash

Kinetic models	Parameters	Unit	Equation non-Linear
Simple first-order			
k_1	0.006	min^{-1}	$C_t = C_0 e^{k_1 t}$
C_0	0.260	mg/L	
R^2	0.952		
Pseudo-second-order k_2			
k_2	0.043	$mg^{-1}\ min^{-1}$	$\frac{dq_t}{dt} = k_2 (q_e - q_t)^2$
q_e	0.055	mg/g	
R^2	0.903		

Fig. 9 shows that the Langmuir model is very close to the experimental data as seen from the R^2 constant, which is 0.998. It can be explained that bottom ash is an adsorbent that absorbs CO_2 in the monolayer at a pressure of 1 atm and a temperature of 25 °C.

Kinetic Studies

An analysis of the kinetic adsorption process is a helpful tool to estimate the time of residence for the adsorption process to complete and determine adsorption dynamics and its performance in the industrial scale of a fixed bed or flow-through system. Thus, the simple first-order and pseudo-second-order models were performed in this study. The kinetic parameters of these models are shown in Table 3. Comparing the values of determination coefficients as stated in Table 3, the simple first-order model gives a better fit than the pseudo-second-order, with an R^2 value is 0.952 [20-23].

■ CONCLUSION

A similar result was supported with FT-IR spectrum at the wavelength 958–954 cm^{-1}, showing that the Si–O–Si group and EDX analysis show silica and oxygen atomic contents were 11.88% and 36.90%, respectively. The CO_2 adsorption efficiency was 70%, while adsorption capacity was 0.350 mg/g at 12 cm bed height operating condition. The isotherm model obtained in this study was Langmuir, while the kinetic model was simple first order. Therefore, bottom ash can be used to capture CO_2 emissions.

■ ACKNOWLEDGMENTS

The author thanks the ministry of Malikussaleh University for financial support through the research project PNBP, No. 530/UN45/KPT/2021.

■ REFERENCES

[1] Abunowara, M., Bustam, M.A., Sufian, S., and Eldemerdash, U., 2016, Description of carbon dioxide adsorption and desorption onto Malaysian coals under subcritical condition, *Procedia Eng.*, 148, 600–608.

[2] Silva, J.A.C., Schumann, K., and Rodrigues., A.E., 2012, Sorption and kinetics of CO_2 and CH_4 in binderless beads of 13X zeolite, *Microporous Mesoporous Mater.*, 158, 219–228.

[3] Kongnoo, A., Tontisirin, S., Worathanakul, P., and Phalakornkule, C., 2017, Surface characteristics and CO_2 adsorption capacities of acid-activated zeolite 13X prepared from palm oil mill fly ash, *Fuel*, 193, 385–394.

[4] Chen, S.J., Zhu, M., Fu, Y., Huang, Y.X., Tao, Z.C., and Li, W.L., 2017, Using 13X, LiX, and LiPdAgX zeolites for CO_2 capture from post-combustion flue gas, *Appl. Energy*, 191, 87–98.

[5] Hauchhum, L., and Mahanta, P., 2014, Carbon dioxide adsorption on zeolites and activated carbon by pressure swing adsorption in a fixed bed, *Int. J. Energy Environ. Eng.*, 5 (4), 349–356.

[6] Girimonte, R., Formisani, B., and Testa, F., 2017, Adsorption of CO_2 on a confined fluidized bed of pelletized 13X zeolite, *Powder Technol.*, 311, 9–17.

[7] Campo, M.C., Ribeiro, A.M., Ferreira, A.F.P., Santos, J.C., Lutz, C., Loureiro, J.M., and Rodrigues A.E., 2016, Carbon dioxide removal for methane

upgrade by a VSA process using an improved 13X zeolite, *Fuel Process. Technol.*, 143, 185–194.

[8] Ridha, F.N., Manovic, V., Macchi, A., and Anthony, E.J., 2015, CO_2 capture at ambient temperature in a fixed bed with CaO-based sorbents, *Appl. Energy*, 140, 297–303.

[9] Gouveia, L.G.T., Agustini, C.B., Perez-Lopez, O.W., and Gutterres, M., 2020, CO_2 adsorption using solids with different surface and acid-base properties, *J. Environ. Chem. Eng.*, 8 (4), 103823.

[10] Regufe, M.J., Ribeiro, A.M., Ferreira, A.F.P., and Rodrigues, A., 2019, "CO_2 storage on zeolites and other adsorbents" in *Nanoporous Materials for Gas Storage, Green Energy and Technology*, Eds. Kaneko, K., and Rodríguez-Reinoso, F., Springer, Singapore, 359–381.

[11] Gil, A., Arrieta, E., Vicente, M.A., and Korili, S.A., 2018, Synthesis and CO_2 adsorption properties of hydrotalcite-like compounds prepared from aluminum saline slag wastes, *Chem. Eng. J.*, 334, 1341–1350.

[12] Bezerra, D.P., da Silva, F.W.M., de Moura, P.A.S., Sousa, A.G.S., Vieira, R.S., Rodriguez-Castellon, E., and Azevedo, D.C.S., 2014, CO_2 adsorption in amine-grafted zeolite 13X, *Appl. Surf. Sci.*, 314, 314–321.

[13] Bezerra, D.P., Silva, F.W.M., de Moura, P.A.S., Sousa, A.G.S., Vieira, R.S., Rodriguez-Castellon, E., Azevedo, D.C.S., 2014, Adsorption of CO_2 on amine grafted activated carbon, *Adsorpt. Sci. Technol.*, 32, 141–151.

[14] Dantas, T.L.P., Luna, F.M.T., Silva, I.J., de Azevedo, D.C.S., Grande, C.A., Rodrigues, A.E., and Moreira, R.F.P.M., 2011, Carbon dioxide–nitrogen separation through adsorption on activated carbon in a fixed bed, *Chem. Eng. J.*, 169 (1-3), 11–19.

[15] Laharto, P.B.F., Anggraini, A.P.K., Fauzany, U.S., Kurniawan, R.Y., and Endang, P.S., 2019, Synthesis of mesoporous silica from bottom ash waste for CH_4 adsorption, *Mater. Sci. Forum*, 964, 130–135.

[16] Liu, Q., He, P., Q, Qian, X., Fei, Z., Zhang, Z., Chen, X., Tang, J., Cui, M., Qiao, X., and Shi, Y., 2017, Enhanced CO_2 adsorption performance on hierarchical porous ZSM-5 zeolite, *Energy Fuels*, 31 (12), 13933–13941.

[17] Lira-Zúñiga, S., Sáez-Navarrete, C., Rodríguez-Córdova, L., Herrera-Zeppelin, L., and Herrera-Urbina, R., 2016, CO_2 adsorption on agricultural biomass combustion ashes, *Maderas, Cienc. Tecnol.*, 18 (4), 607–616.

[18] Lee, S.Y., and Park, S.J., 2015, A review on solid adsorbents for carbon dioxide capture, *J. Ind. Eng. Chem.*, 23, 1–11.

[19] Sylvia, N., Mutia, R., Malasari, M., Dewi, R., Bindar, Y., and Yunardi, Y., 2019, A computational fluid dynamic comparative study on CO_2 adsorption performance using activated carbon and zeolite in a fixed bed reactor, *IOP Conf. Ser.: Mater. Sci. Eng.*, 536, 012042.

[20] Yoro, K.O., Singo, M., Mulopo, J.L., and Daramola, M.O., 2017, Modelling and experimental study of the CO_2 adsorption behaviour of polyaspartamide as an adsorbent during post-combustion CO_2 capture, *Energy Procedia*, 114.

[21] Lakapu, M.M., and Widiastuti, N., 2017, Synthesis of zeolite-X supported on kapok fiber for CO_2 capture material: Variation of immersion time during fiber activation, *Indones. J. Chem.*, 17 (3), 471–476.

[22] Haider, M.B., Jha, D., Sivagnanam, B.M., and Kumar, R., 2018, Thermodynamic and kinetic studies of CO_2 capture by glycol and amine-based deep eutectic solvents, *J. Chem. Eng. Data*, 63 (8), 2671–2680.

[23] Ghazali, Z., Yarmo, M.A., Hassan, N.H., Teh, L.P., and Othaman, R., 2020, New green adsorbent for capturing carbon dioxide by choline chloride: Urea-confined nanoporous silica, *Arabian J. Sci. Eng.*, 45 (6), 4621–4634.

[24] Wardani, A.R.K., and Widiastuti, N., 2016, Synthesis of zeolite-X supported on glasswool for CO_2 capture material: Variation of immersion time and NaOH concentration at glasswool activation, *Indones. J. Chem.*, 278, 16 (1), 1–7.

[25] Minzatu, V., Adina, N., Davidescu, C.M., Duda, C.S., Ciopec, M., Duteanu, N., Negrea, P., Seiman, D.D., and Pascu, I., 2018, Arsenic adsorption into the fixed bed column from drinking groundwater, *WIT Trans. Ecol. Environ.*, 228, 101–110.